Polym. Bull. (2012) 68:375–390
DOI 10.1007/s00289-011-0544-6

ORIGINAL PAPER

Clay-reinforced semi-aromatic polyether-amide nanocomposites containing phosphine oxide moieties: synthesis and characterization

Meisam Shabanian · Khalil Faghihi · Fatemeh Shabani

Received: 28 November 2010 / Revised: 3 June 2011 / Accepted: 3 June 2011 /
Published online: 12 June 2011

Abstract Semi-aromatic flame retardant polyether-amide/organoclay nanocomposites were synthesis through solution blending technique. Surface modification of the montmorillonite clay was performed with 1,4-bis[4,4′-amino phenoxy]butane for ample compatibilization with the polyamide matrix. The polymer chains were produced from the poly condensation reaction of bis(3-amino phenyl)phenyl phosphine oxide (4) with 1,4-(4-carboxy phenoxy)butane (3). The effect of clay dispersion and the interaction between clay and polyamide chains on the properties of nanocomposites were investigated using X-ray diffraction, scanning electron microscopy, limited oxygen index, differential scanning calorimetry, thermogravimetric analysis, and water uptake measurements. The diacid 3 as a monomer was prepared from the reaction of 4-hydroxy benzoic acid (1) with 1,4-dibromo butane (2) in the presence of NaOH solution.

Keywords Nanocomposites · Flame-retardant polymers · Organoclay · Polyamide

Introduction

Polymer–clay nanocomposites have received significant attention, since the first report of polyamide-6-clay nanocomposites by Toyota's research group in 1990 [1]. Subsequent studies have discovered that physical and chemical properties of organic polymers, such as thermal stability, [2] mechanical strength, [3] solvent resistance, [4] flame retardation, [5] ionic conductivity, [6] corrosion resistance, [7] gas barrier properties, [8], and dielectric properties [9] are substantially improved by the introduction of small portions of inorganic clay. Performance of polymer–clay

M. Shabanian · K. Faghihi (✉) · F. Shabani
Organic Polymer Chemistry Research Laboratory, Department of Chemistry, Faculty of Science, Arak University, 38156-8-8349 Arak, Iran
e-mail: k-faghihi@araku.ac.ir

nanocomposites strongly depends on dispersion and spacing between clay layers. According to the distance between layers, the polymer–clay nanocomposites can be divided into two categories: intercalated and exfoliated [1]. The enhancements of physical and chemical properties occur even with the addition of low percentages of organically modified clay; the properties are maximized when the clay platelets are exfoliated and randomly dispersed in a polymer matrix.

Aromatic polyamides possess excellent mechanical properties and thermal stability; however, they are difficult to process because of limited solubility and high glass transition (T_g) or melt temperature due to chain stiffness and intermolecular hydrogen bonding between amide groups [10]. The processing of these thermoplastic polymers has been greatly hindered because they lack softening or melting behavior at usual processing temperature, and they tend to degrade before or at the softening temperature [11]. Various attempts have been made to bring down the T_g or melting temperature of aromatic polyamides to make them processable, either by introducing linked and flexible bridging units [12–14] into the polymers chain. Unfortunately, the loss of thermal stability and significant decrease in mechanical properties on heating are usually a consequence of the reduced chain stiffness. Much effort has been made to create structurally modified aromatic polymers having increased solubility and processability with retention of their high thermal stability. It is known that the solubility of polymers is often increased when flexible bonds such as [–O–, $–SO_2–$, $–CH_2–$, $–C(CF_3–)_2$], bulky pendent groups (such as t-butyl and adamantyle), large pendent groups or polar constituents are incorporated into the polymer backbone due to the altering crystallinity and intermolecular interactions [15–19]. It has been recognized that the incorporation of aryl-ether linkages generally imparts an enhanced solubility, processability, and toughness of aromatic polyamides and polyimides as well as their copolymers without substantial diminution of thermal properties [20].

A variety of flame retardant polymers have been developed over the past 20 years, and many of these are suitable for use in fiber composites. The incorporation of bromine, chlorine, or phosphorus into the molecular structure of a polymer is the most common method used to improve the flammability resistance of thermoset resins and thermoplastics. Among the polymers with phosphorus moieties, the polymers with phosphine oxide moieties have major advantages, such as good flame-retardant properties, high thermal oxidative stability, enhanced solubility in organic solvents, improved miscibility, and good adhesion to other compounds. The incorporation of nano-sized particles into a resin is another approach for improving fire resistance. Polymer nanocomposites are rapidly emerging as an important class of flame retardant materials. Polymer–clay nanocomposites have not only the advantage of reduced flammability, but they also exhibit improved mechanical properties. This is a key advantage, because many fire retardants are used at relatively high loadings and this may lead to a significant reduction in the mechanical properties of the polymer [14, 21, 22].

In this study a new aromatic-aliphatic polyamide containing ether linkages and phosphine oxide moieties was prepared by direct polycondensation method that could offer a balance of properties between those of tractable aliphatic nylons and the virtually insoluble and non-melting wholly aromatic polyamides. This

aromatic–aliphatic polyamide is soluble in DMF, DMSO, and DMAc which can be attributed to the flexible ether linkages and the polyamide was reinforced with reactive montmorillonite intercalated with diamine species. The nanocomposites obtained by solution intercalation technique were characterized for XRD, SEM, LOI, TGA, DSC, and water uptake measurements.

Experimental

Materials

All chemicals were purchased from Merck Chemical Co. (Germany) and Aldrich (USA).

Instruments

^{1}H NMR spectra were recorded on a Bruker 300 MHz instrument. Fourier transform infrared (FTIR) spectra were recorded on Galaxy series FTIR 5000 spectrophotometer (England). Spectra of solids were performed by using KBr pellets. Vibrational transition frequencies are reported in wave number (cm^{-1}). Band intensities are assigned as weak (w), medium (m), shoulder (sh), strong (s), and broad (br). Inherent viscosities were measured by a standard procedure using a Technico® Merk Viscometer. Limited oxygen indexes (LOI) were measured on a Stanton Redcraft flamemeter. Thermal gravimetric analysis (TGA and DTG) data for polymers were taken on a Mettler TA4000 System under N_2 atmosphere at a rate of 10 °C/min. differential scanning calorimeter (DSC) was conducted with a DSC Metller 110 (Switzerland) at a heating rate of 10 °C/min in a nitrogen atmosphere. The morphology of nanocomposite film was investigated on Canbridge S260 scanning electron microscope (SEM). X-ray diffraction (XRD) were performed on Philips X-Pert (Cu–Ka radiation, $\lambda = 0.15405$ nm). The water absorption of PA-nanocomposite films were carried out using a procedure under ASTM D570-81 [23].

Monomer synthesis

1,4-(4-carboxy phenoxy)butane (3)

In a 250-mL round-bottomed flask with dropping funnel fitted with a stirring bar were placed (4.60 g, 33.3 mmol) of 4-hydroxy benzoic acid (1) and (2.60 g, 65.0 mmol) sodium hydroxide in 14.0 mL H_2O. Then (3.62 g, 16.8 mmol) 1,4-dibromo butane (2) was added into the reaction mixture slowly with stirring and the reaction mixture was refluxed for 3.5 h. After that (0.66 g, 16.5 mmol) NaOH was added and refluxing continuing for 2 h. Then the heating was removed, the stirring continued at room temperature for over night. After that the white precipitate was filtered and washed with 10 mL methanol, the solid was dissolved in 34 mL H_2O. By adding a solution of H_2SO_4 (6 N) a white solid was precipitate, washed with the

cold water and filtered at room temperature until 3.94 g (71%) white product was obtained. m.p: 328–330 °C, FTIR (KBr): 2400–3500 (s, br), 1689 (s, br), 1606 (s), 1514 (s), 1429 (s), 1300 (w), 1220 (m), 1172 (m), 1110 (w), 1049 (s), 972 (m), 848 (s), 773 (s), 696 (m), 646 (m), 594 (m), 505 (m) cm^{-1}. ^{1}H NMR (DMSO-d_6, TMS) δ: 1.89 (s, 4H), 4.10 (s, 4H), 7.00–7.02 (d, 4H), 7.85–7.89 (d, 4H), 12.60 (s, br, 2H) ppm. ^{13}C NMR (300 MHz, DMSO-d_6): δ; 167.4, 162.6, 131.8, 123.3, 114.6, 67.8, 25.6 ppm. Elemental analysis: calculated for $C_{18}H_{18}O_6$: C, 65.45; H, 5.49; found: C, 65.21; H, 5.42.

Bis(3-amino phenyl) phenyl phosphine oxide (4)

This compound was prepared according to our previous works [24]

1,4-Bis[4,4′-aminophenoxy]butane (BAB)

The diamine was prepared according to our previous works [25]

Preparation of preparation of BAB–MMT

Organophilic (MMT) was prepared by cation exchange of sodium ions within (MMT) clay with alkylammonium ions of the intercalation agent. Typically, 5 g of (MMT) clay was stirred in 600 mL of distilled water (beaker A) at room temperature overnight. A separate solution containing 1.5 g of (BAB) in 30 mL of distilled water (beaker B) was prepared with the aid of magnetic stirring and the addition of a 1.0 mol L^{-1} HCl aqueous solution to adjust the pH value to 3–4. After stirring for 3 h, the protonated diamine solution (beaker B) was added to the (MMT) suspension (beaker A) at a rate of approximately 10 mL min^{-1} with vigorous stirring. The mixture was stirred overnight at room temperature. Organophilic (MMT) was filtering using a Buchner funnel. The resulting organophilic (MMTs) were washed and filtered at least four times to remove any excess ammonium ions.

Polymer synthesis

In a 25-mL round-bottomed flask which was fitted with a stirring bar were placed bis(3-amino phenyl) phenyl phosphine oxide (4) (0.197 g, 0.64 mmol), diacid (3) (0.211 g, 0.64 mmol), calcium chloride (0.20 g, 1.80 mmol), triphenyl phosphite (1.68 mL, 6.00 mmol), pyridine (0.36 mL) and *N*-methyl-2-pyrrolidone (1.6 mL). The reaction mixture was heated under reflux on an oil bath at 60 °C for 1 h, then 90 °C for 2 h, and 130 °C for 6 h. To the reaction contents, 1% of diacid (3) was added in order to generate acid group terminal ends and reflux was continue for 2 h. The polyether-amide formed was viscous, then the reaction mixture was poured into 50 mL of methanol and the precipitated polymer was collected by filtration and washed thoroughly with hot methanol and dried at 60 °C for 12 h under vacuum to leave 0.35 g (93%) of brown solid polymer (5). The inherent viscosity of the soluble PEA is 0.69 dL/g.

Synthesis of semi-aromatic polyamide/BAB–MMT nanocomposites

The nanocomposites were prepared by mixing the appropriate amounts of the polymer and organoclay in a flask for a particular concentration. The reaction mixture was agitated to high speed stirring at 80 °C for 1 h and then at 25 °C for 24 h for uniform dispersion of clay platelets in the polyamide matrix. Various compositions ranging from 0 to 15 wt% of organoclay were prepared by mixing various amounts of (BAB–MMT) to the polymer solution. Thin composite films of uniform thickness were obtained by pouring the hybrid solutions into petri dishes, followed by solvent evaporation at high temperature. These films were further dried at 80 °C under reduced pressure to a constant weight.

Results and discussion

Monomer synthesis

1,4-(4-Carboxy phenoxy)butane (3) was prepared from the reaction of 4-hydroxy benzoic acid (1) with 1,4-dibromo butane (2) in the presence of NaOH solution (Scheme 1).

The chemical structure and purity of diacid (3) was proved with elemental analysis, ^{1}H NMR, and FTIR spectroscopy. The measured results in elemental analyses of compound (3) closely corresponded to the calculated ones, demonstrating that the expected compound was obtained. The FTIR spectrum of compound (3) showed a broad peak between 2400 and 3500 cm^{-1}, which was assigned to the COOH groups.

The ^{1}H NMR spectrum of compound (3) showed a broad singlet peak at 12.60 ppm which was assigned to the H(a) protons of the COOH groups. Two doublet peaks between 7.00–7.02 and 7.85–7.89 ppm which were assigned to the H(b) and H(c) protons of the phenyl ring. Furthermore two singlet peaks at 4.10 and 1.89 ppm were assigned to the aliphatic protons of the methylene groups (Fig. 1).

Figure 2 displays ^{13}C NMR spectrum of dicarboxylic acid (3), that this spectrum showed seven different signals for carbon atoms. Carbon atoms for acidic carbonyl group appeared in 166.24 ppm. Carbon atoms related to aromatic appeared in the

Scheme 1 Synthesis of diacid (**3**)

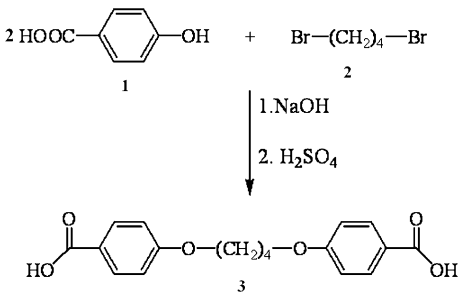

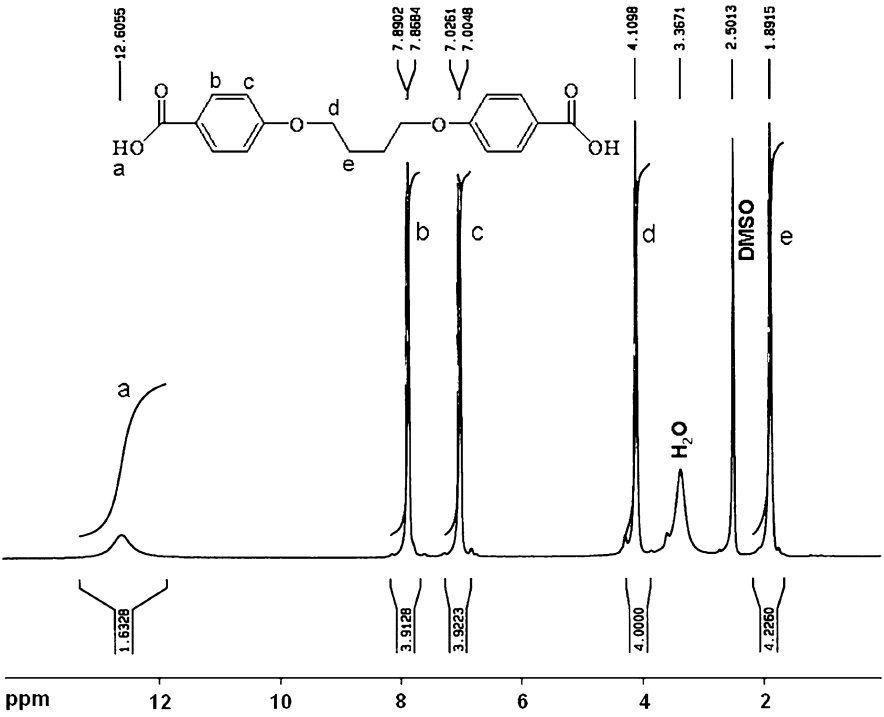

Fig. 1 ^{1}H NMR spectrum of diacid (**3**)

range of 114–162 ppm. These peaks in ^{1}H NMR and ^{13}C NMR spectra along with elemental analyses data confirmed the proposal structure of the dicarboxylic acid.

Bis(3-aminophenyl)phenyl phosphine oxide (4) was prepared by using a three step reaction from the simple organic compounds such as triphenyl phosphine. At first triphenyl phosphine was oxidized to triphenyl phosphine oxide, then compound 2 was converted to bis(3-nitrophenyl) phenyl phosphine oxide by using concentrated nitric acid in the presence of sulfuric acid. Bis(3-nitrophenyl) phenyl phosphine oxide was reduced to bis(3-aminophenyl) phenyl phosphine oxide (4) with $SnCl_2{\cdot}2H_2O$.

Also 1,4-bis[4,4′-aminophenoxy]butane (BAB) as a swilling agent was synthesized by using a two-step reaction. At first 1,4-bis[4,4′-nitrophenoxy]butane was prepared from the reaction of two equimolars 4-nitrophenol and one 1,4-dibromo butane in DMF and dry K_2CO_3. Then dinitro compound was reduced by using 10% Pd–C, ethanol, and hydrazine monohydrate.

Polymer synthesis

PEA was synthesized by the direct polycondensation reaction of an equimolar mixture of diacid (3) with the diamine (4) in a medium consisting of *N*-methyl-2-pyrrolidone, triphenyl phosphite, calcium chloride, and pyridine (Scheme 2).

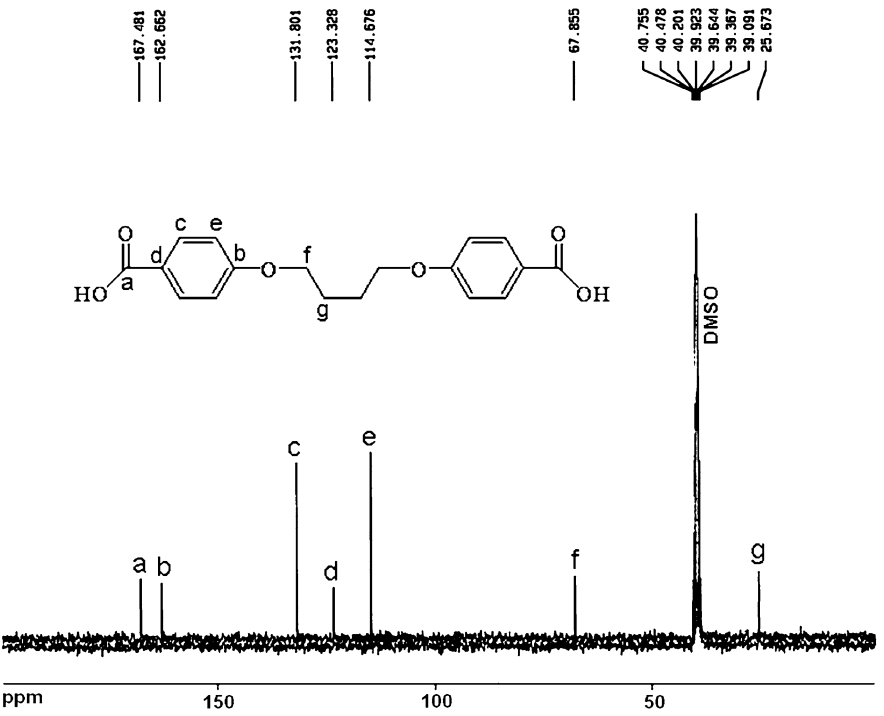

Fig. 2 ^{13}C NMR spectrum of diacid (**3**)

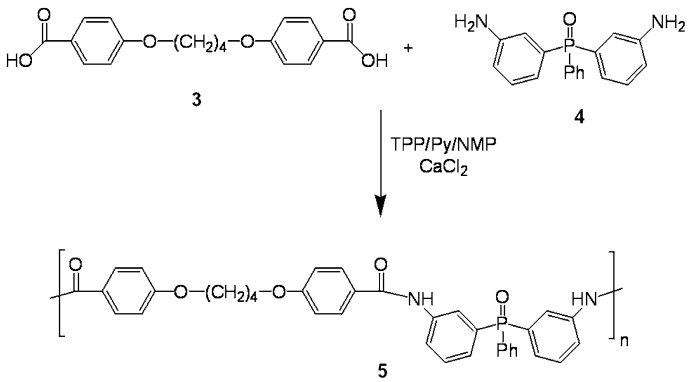

Scheme 2 Synthesis of PEA (**5**)

Polymer nanocomposite synthesis

MMT has a high swelling capacity, which is important for efficient intercalation of the polymer, and is composed of stacked silicate sheets that boost many properties of bulk polymers. In this study, the preparation of composites can be classified into the following two steps. First, organic soluble polyether-amide is first prepared by

direct amidation process. Second, the organophilic clay is dispersing into the PEA matrix by the solution dispersion technique. The preparation flowchart of soluble PEANs materials by direct amidation is given in Scheme 3.

Polymer characterization

The structures of the polymers were confirmed as PEA by means FTIR and ^{1}H NMR spectroscopy.

The ^{1}H NMR spectrum of PEA (5) showed peaks that confirm its chemical structure (Fig. 3). The aromatic protons related to the polymer appeared in the

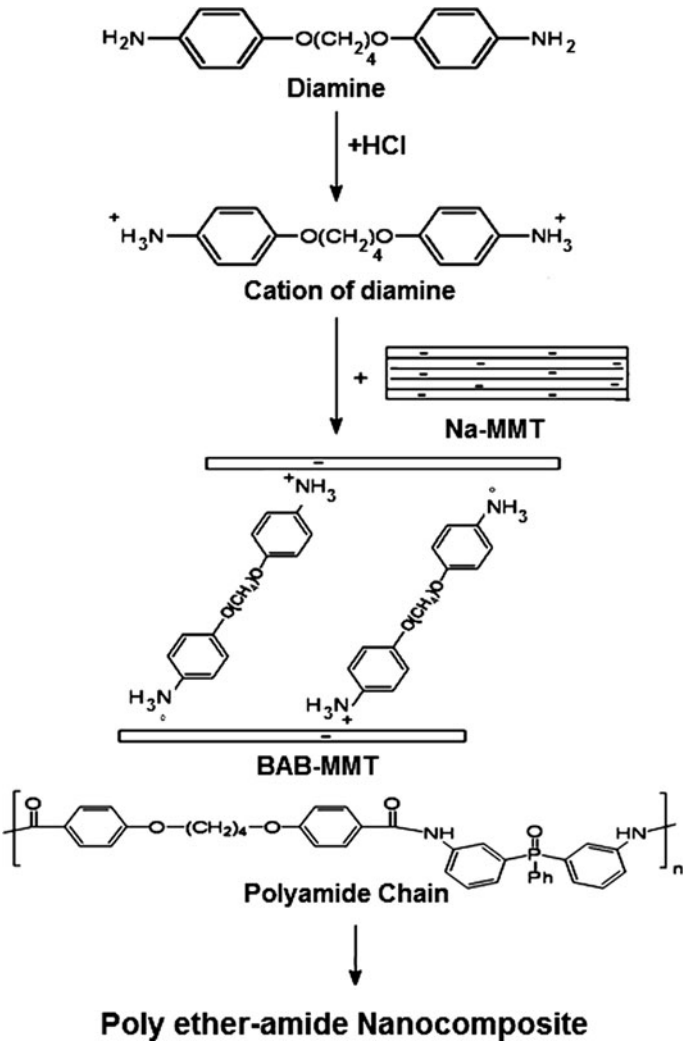

Scheme 3 Synthesis of PEANs

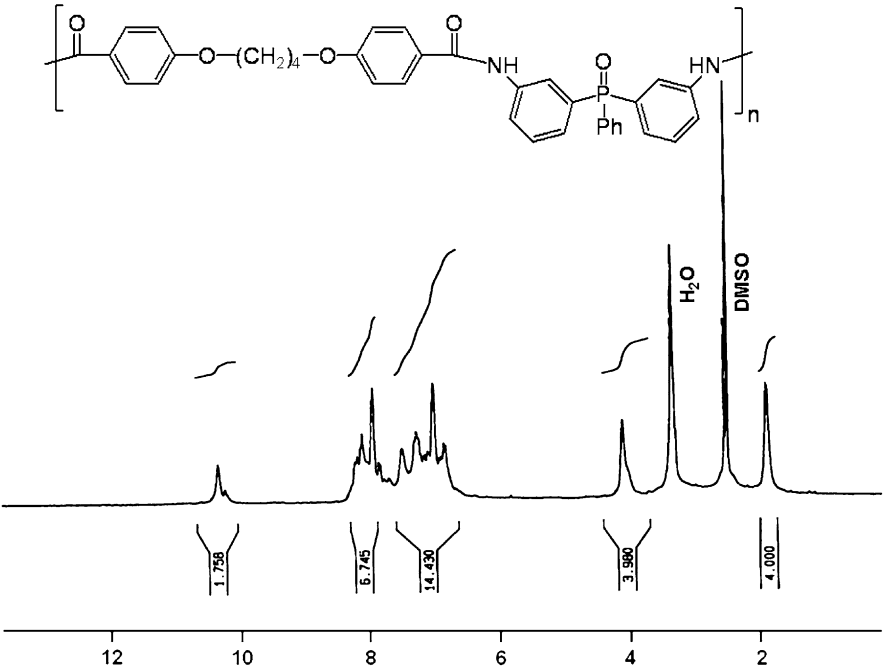

Fig. 3 ^{1}H NMR spectrum of PEA (**5**)

region of 6.83–8.22 ppm and the peak in the region of 10.34 ppm is assigned for N–H of amide groups in the main chain of polymer. Decaying peak related to carboxylic acid protons and appearing peaks related to amide groups and aromatic protons of diamine in the polymer chain, confirmed the proposed structure of PEA.

FTIR characterizations of the PEA and PEANs are listed in Table 1. Figure 4 shows the representative FTIR spectrum for PEAN5%. The characteristic vibration bands of amide groups (C=O stretching vibration) are shown at 1662 cm^{-1} related to The absorption bands of amide groups appeared at 3321 cm^{-1} (N–H stretching) and MMT clay at 1040 cm^{-1} (Si–O), 523 cm^{-1} (Al–O), and 464 cm^{-1} (Mg–O). As the loading of MMT clay was increased, the intensity of MMT clay bands became much stronger in the FTIR spectra of PEANs materials.

X-ray diffraction

Dispersion of organoclay in the nanocomposites was monitored by XRD taken at low 2θ region and the results are narrated in Fig. 5. The neat MMT clay gives a distinct peak around 2θ equal to 8.88. The organically modified MMT employed for the preparation of nanocomposites has a typical peak at 2θ equal to 6.61 that relates to a peak of (BAB–MMT) confirming that MMT turns out to be organophilic with increased d-spacing. In hybrid films containing 5 wt% organoclay, the peak of BAB–MMT occurring at $2\theta = 6.61$ was absent, which indicated dispersion of ordered platelets of the clay and verified delamination of nanolayers in the matrix (Fig. 5).

Table 1 FTIR charcterization of PEANs

BAB-MMT Contents (%)	Spectral data
0.0	*FTIR Peaks (cm^{-1})* 3308 (m), 3055 (w), 2947 (w), 1666 (s), 1604 (s), 1508 (s), 1410 (m), 1309 (m), 1244 (s), 1174 (m), 1080 (m), 995 (w), 895 (m), 761 (m), 690 (m), 501 (m).
5.0	*FTIR Peaks (cm^{-1})* 3319 (m), 2920 (m), 1677 (s), 1514 (s), 1473 (m), 1321 (w), 1298 (w), 1248 (s), 1170 (m), 1120 (w), 1049 (m), 1041 (w), 977 (w), 867 (m), 761 (m), 615 (w), 526 (m), 464 (w).
10.0	*FTIR Peaks (cm^{-1})* 3310 (m), 1669 (m), 1605 (s), 1514 (s), 1472 (m), 1410 (w), 1309 (m), 1220 (m), 1181 (w), 1072 (m), 1040 (w), 940 (w), 688 (w), 523 (m), 462 (m).
15.0	*FTIR Peaks (cm^{-1})* 3311 (m), 3041 (w), 1666 (s), 1604 (m), 1502 (s), 1404 (w), 1302 (w), 1220 (w), 1172 (w), 1082 (w), 1143 (w), 937 (w), 760 (m), 690 (w), 520 (m), 462 (m).

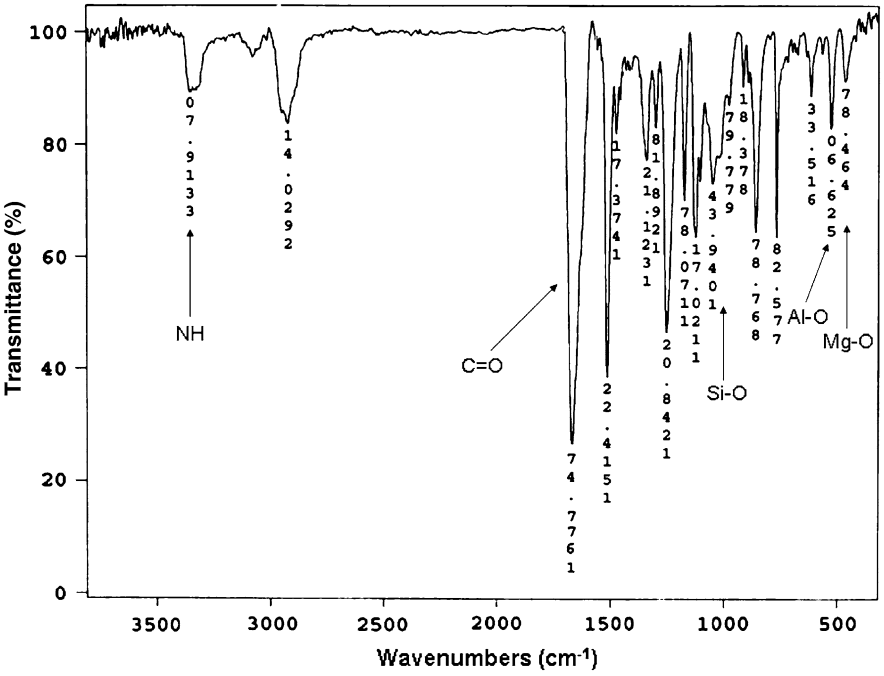

Fig. 4 FTIR spectrum of PEAN 5%

When the amount of organoclay increased (10, 15 wt%) in the nanocomposites, small peaks appeared at $2\theta = 6.18$ and 6.10, respectively. This XRD pattern confirmed both delaminated and intercalated structures of MMT. Dispersion of clay in the composites depends on the type of swelling agent and its interaction with the polymer chains. The amine end group of swelling agent interacted ionically with silicate layers and develops interactions with acid end-capped polyamide chains

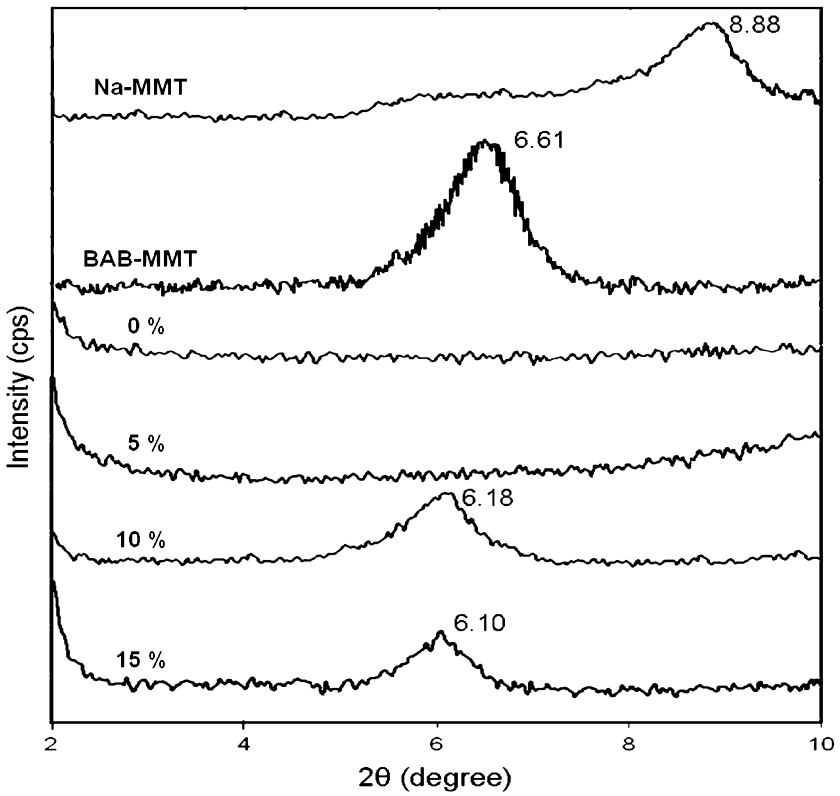

Fig. 5 XRD pattern of semi-aromatic PEA/BAB–MMT nanocomposites

diffused into the interlayer of clay. Such interactions result a finite interlayer expansion when polyamide chains intercalated into the interlayer of clay, polyamide's transitional entropy increases while its conformational entropy decreases, but at the same time, the modified clay gains conformational entropy. The fine dispersion of nanolayers depends on both entropic and enthalpic contributions of the system, which are related to the properties of polymer and modified clay. Polyamide being a polar polymer made the enthalpic translation between the polymer and modified clay much easier so that the chains of polyamide intercalated into the interlayers of clay.

Scanning electron microscopy

SEM micrographs of fractured surface of the nanocomposites are presented in Fig. 6. These images did not exhibit inorganic domains at the maximum possible magnification, which means nanolayers are distributed well in the polyamide matrix. The absence of MMT particles indicates that the agglomerate is broken down to a size (submicron) that cannot be seen at this magnification.

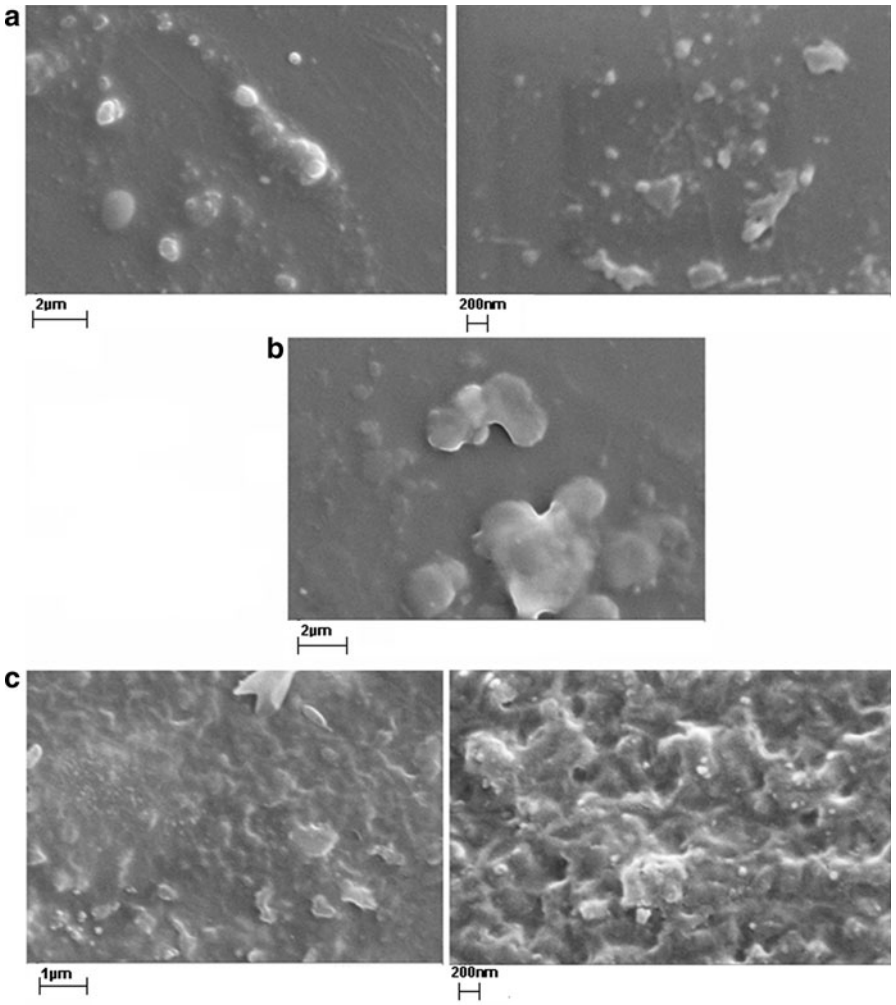

Fig. 6 SEM micrographs of semi-aromatic PEA/BAB–MMT nanocomposites: **a** 5 wt% **b** 10 wt%, and **c** 15 wt%

Thermogravimetric analysis

Thermal stability of the polyamide/oligomer-MMT composites determined under inert atmosphere is shown in Fig. 7. The initial decomposition temperatures of 5 and 10% weight losses (T_5 and T_{10}) and the char yield at 800 °C are summarized in Table 2. Thermal decomposition temperatures of the nanocomposites were found in the range 300–400 °C. Thermograms indicated that nanocomposites are thermally stable, which increased with the addition of oligomer-MMT in the polyamide. Nanocomposites prepared from polyamides and different ceramic phases showed enhanced thermal stability upon the addition of these inorganic materials. The weight retained at 800 °C is roughly proportional to the amount of organoclay in the

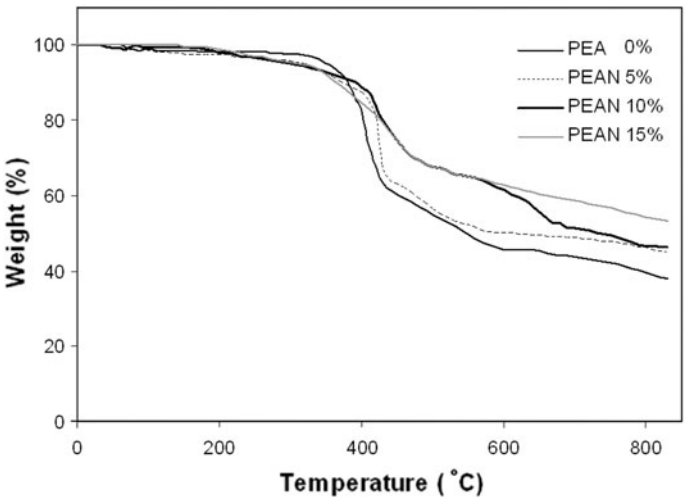

Fig. 7 TGA curves of PEANs

nanocomposites. Inclusion of the inorganic filler into the organic phase was found to increase the thermal stability presumably due to superior insulating features of the layered silicate which also acts as mass transport barrier to the volatile products generated during decomposition.

Also the flame retardant property of these polymers was evaluated by measuring their LOI values. They showed LOI data between 32 and 36.

Generally, materials exhibiting LOI values greater than 26 would show self-extinguishing behavior [26] and were considered to be flame retardant. Therefore, high char yield data, along with good LOI values between 32 and 36, indicated that these polymers have good flame retardant properties.

The char yield can be applied as a decisive factor for estimated the limiting oxygen index (LOI) of polymers according to the equation of Van Krevelen and Hoftyzer [27]:

$$\mathrm{LOI} = 17.5 + 0.4\mathrm{CR}$$

where CR is the char yield.

The PEANs had LOI values between 33 and 39, which were calculated from their char yield. On the basis of the LOI values, such macromolecules can be classified as self-extinguishing polymers.

Differential scanning calorimetry

The glass transition temperatures of nanocomposites were recorded using DSC technique that increased with augmenting organoclay contents (Table 2). These results described a systematic increase in the T_g values as a function of organoclay showing greater interaction between the two disparate phases. The maximum T_g value (192 °C) was obtained with 15 wt% addition of organoclay relative to pristine

Table 2 Thermal behavior and water absorption measurements of PEANs

BAB–MMT contents (%)	T_g[a]	T_5(°C)[b]	T_{10}(°C)[b]	Char yield[c]	LOI	LOI[d]	Water uptake at equilibrium (%)
0.0	165	350	380	39.43	32	33	14.5
5.0	180	315	375	46.22	35	36	11.2
10.0	190	300	390	46.67	35	36	8.7
15.0	192	310	365	54.12	36	39	2.8

LOI limited oxygen index

[a] Glass transition temperature was recorded at a heating rate of 10 °C min^{-1} in a nitrogen atmosphere

[b] Temperature at which 5 or 10% weight loss was recorded by TGA at a heating rate of 10 °C/min under N_2

[c] Weight percentage of material left after TGA analysis at a maximum temperature of 800 °C under N_2

[d] Calculated by equation of Van Krevelen and Hoftyzer

polyamide (165 °C). Further inclusion of the (BAB–MMT) decreased the T_g because the entire clay may not interact with the polymer matrix resulting in poor interfacial interactions. Introduction of modified clay impeded the segmental motion of the polymer chains and increased amount of organoclay shifted the baseline of DSC curve toward higher temperature. This also suggested that polyamide chains developed interactions with organophilic silicate layers. As a result, the motions of polymer chains were restricted, thereby, increasing the T_g values of the composite materials. Glass transition temperatures of nanocomposites increased for all the compositions studied. The change of glass transition temperature of the polymer composites relative to pure polyamide is attributed to the interaction between the filler and matrix at interfacial zones.

Water absorption measurements

The presence of silicate layers may be expected to decrease the water uptake due to a more tortuous path for the diffusing molecules that must bypass impenetrable platelets.

The improved barrier characteristics, chemical resistance, reduced solvent uptake, and flame retardance of clay–polymer nanocomposites take advantage from the hindered diffusion pathways through the nanocomposite. The water uptake of composite materials measured under the saturation conditions (168 h) are shown in Table 2. The results showed maximum water absorption for the neat polyamide film 14.5% due to exposure of amide groups to the surface of polymer where water molecules developed secondary bond forces with these polar groups. The increase in weight of the hybrid films due to uptake of water gradually decreased as the organoclay content in nanocomposites increased. This decrease is apparently due to the mutual interaction between the organic and inorganic phases. This interaction resulted in lesser availability of amide to interact with water.

Conclusion

The new polyamide containing phosphine oxide and ether moiety was synthesis and used as a source of polymeric matrix. Flexible groups from the diacid (ether and alkylene groups) increased the solubility of the polymers in organic solvents. The incorporation of modified clay reinforces the polyamide matrix, depicting compatibility between the polymer and clay. Chemical interaction produced between organic and inorganic phases result in uniformly dispersed BAB–MMT throughout the matrix. The functionality of the swelling agent was adjusted in such a way that one of the amine ends formed an ionic bond with negatively charged silicates and the other free amino group in the modifier is available for further reaction with carbonyl chloride end-capped polyamide. At 15 wt% BAB–MMT loading, the dispersion of individual silicate sheet is optimum, giving an observed increase in the thermal stability and flame retardancy of these materials. These thermally stable composites also exhibit considerable increase in T_g values and reduction in the water absorption. Flame retardancy, thermal stability and organosoluble properties can make these nanocomposites attractive for practical applications such as processable high-performance engineering plastics.

References

1. Lai MC, Jang CG, Chang KC, Hsu SC, Hsieh MF, Yeh JM (2008) Comparative studies for the effect of dual- and mono-organic modifiers on the physical properties of polyimide-clay nanocomposite membranes. J Appl Polym Sci 109:1730–1737
2. Lan T, Kaviratna PD, Pinnavaia TJ (1994) On the nature of polyimide-clay hybrid composites. Chem Mater 6:573–575
3. Tyan HL, Liu YC, Wei KHT (1999) Thermally and mechanically enhanced clay/polyimide nanocomposite via reactive organoclay. Chem Mater 11:1942–1947
4. Burnside SD, Giannelis EP (1995) Synthesis and properties of new poly(dimethylsiloxane) nanocomposites. Chem Mater 7:1597–1600
5. Gilman JW, Jackson CL, Morgan AB, Hayyis R Jr, Manias E, Giannelis EP, Wuthenow M, Hilton D, Philips SH (2000) Flammability properties of polymer-layered-silicate nanocomposites. Polypropylene and polystyrene nanocomposites. Chem Mater 12:1866–1873
6. Vaia RA, Vasudevan S, Krawiec W, Scanlon LG, Giannelis EP (1995) New polymer electrolyte nanocomposites: melt intercalation of poly(ethylene-oxide) in mica-type silicates. Adv Mater 7:154–156
7. Yu YH, Yeh JM, Liou SJ, Chang YP (2004) Organo-soluble polyimide (TBAPP–OPDA)/clay nanocomposite materials with advanced anticorrosive properties prepared from solution dispersion technique. Acta Mater 52:475–486
8. Messersmith PB, Giannelis EP (1995) Synthesis and barrier properties of poly(ε-caprolactone)-layered silicate nanocomposites. J Polym Sci Part A Polym Chem 33:1047–1057
9. Koo CM, Kim SO, Chung IJ (2003) Study on morphology evolution, orientational behavior, and anisotropic phase formation of highly filled polymer-layered silicate nanocomposites. Macromolecules 36:2748–2757
11. Saxena A, Rao VL, Prabhakaran PV, Ninan KN (2003) Synthesis and characterization of polyamides and poly(amide-imide)s derived from 2,2-bis(4-aminophenoxy) benzonitrile. Eur Polym J 39: 401–405
12. Bottino FA, Di Pasquale G, Pollicino A, Scalia L (1999) Synthesis and characterization of new polyamides and copolyamides containing 6,6′-sulfonediquinoline units. Polym Bull 42:519–526

13. Yang CP, Chen YP, Woo EM (2004) Thermal behavior of 1,4-bis(4-trimellitimido-2-trifluoromethyl phenoxy)benzene (DIDA) solvated with polar organic solvents and properties of DIDA-based poly(amide-imide)s. Polymer 45:5279–5293
14. Ge Z, Yang S, Tao Z, Liu J, Fan L (2004) Synthesis and characterization of novel soluble fluorinated aromatic polyamides derived from fluorinated isophthaloyl dichlorides and aromatic diamines. Polymer 45:3627–3635
15. Faghihi Kh, Hajibeygi M, Shabanian M (2009) Synthesis and properties of novel flame-retardant and thermally stable poly(amide-imide)s from N,N′-(bicyclo[2,2,2]oct-7-ene-tetracarboxylic)-bis-L-amino acids and phosphine oxide moiety by two different methods. Macromol Res 17:739–745
16. Faghihi Kh, Hajibeygi M, Shabanian M (2010) Photosensitive and optically active poly(amide-imide)s based on N,N-(pyromellitoyl)-bis-L-amino acid and dibenzalacetone moiety in the main chain: synthesis and characterization. J Macromol Sci Part A Pure App Chem 47:144–153
17. Diakoumakos CD, Mikroyannidis JA (1994) Polyisophthalamides with pendent phthalimide groups. Polymer 35:1986–1990
18. Faghihi Kh, Hajibeygi M, Shabanian M (2010) Novel thermally stable poly(amide-imide)s containing dibenzalacetone moiety in the main chain: synthesis and characterization. Macromol Res 18:421–428
19. Faghihi Kh, Shabanian M, Emamdadi N (2010) Synthesis, characterization and thermal properties of new organosoluble poly(ester-imide)s containing ether group. Macromol Res 18:753–758
20. Faghihi Kh, Shabanian M, Hajibeygi M (2009) Optically active and organosoluble poly(amide-imide)s derived from N,N′-(Pyromellitoyl)bis-L-histidine and various diamines: synthesis and characterization. Macromol Res 17:912–918
21. Zulfiqar S, Kausar A, Rizwan M, Muhammad MI (2008) Probing the role of surface treated montmorillonite on the properties of semi-aromatic polyamide/clay nanocomposites. Appl Surf Sci 255:2080–2086
22. Mouritz AP, Gibson AG (2006) Fire properties of polymer composite materials. Springer, Dordrecht
23. Lee J, Takekoshi T, Giannelis EP (1997) Fire retardant polyetherimide nanocomposites. In: Proceedings of the materials research society symposium (nanophase and nanocomposite materials II), Pittsburgh, 457: 513–518
24. Zulfiqar S, Sarwar MI (2008) Inclusion of aramid chains into the layered silicates through solution intercalation route. J Incl Phenom Macrocycl Chem 62:353–361
25. Faghihi Kh, Zamani Kh (2006) Synthesis and properties of novel flame-retardant poly(amide-imide)s containing phosphine oxide moieties in main chain by microwave irradiation. J Appl Polym Sci 101:4263–4269
26. Faghihi Kh, Shabanian M, Hajibeygi M, Mohammadi Y (2010) Synthesis and properties of new thermally stable and optically active organosoluble poly(ether-amide-imide)s containing bicyclo segment in the main chain. J Appl Polym Sci 117:1184–1192
27. Liu YL, Chiu YC, Chen TY (2003) Phosphorus-containing polyaryloxydiphenylsilanes with high flame retardance arising from a phosphorus-silicon synergistic effect. Polym Int 52:1256–1261
28. Van Krevelen DW, Hoftyzer PJ (1976) Properties of polymer. Elsevier Scientific Publishing Company, New York